The Impact of TRMM Data on Mesoscale Numerical Simulation of Supertyphoon Paka

ZHAOXIA PU

Goddard Earth Sciences and Technology Center, University of Maryland, Baltimore County, Baltimore, and Laboratory for Atmospheres, NASA Goddard Space Flight Center, Greenbelt, Maryland

WEI-KUO TAO, SCOTT BRAUN, AND JOANNE SIMPSON

Laboratory for Atmospheres, NASA Goddard Space Flight Center, Greenbelt, Maryland

YIQIN JIA

Laboratory for Atmospheres, NASA Goddard Space Flight Center, Greenbelt, and Science System and Applications, Inc., Lanham, Maryland

JEFFREY HALVERSON AND WILLIAM OLSON

Laboratory for Atmospheres, NASA Goddard Space Flight Center, Greenbelt, and Joint Center of Earth System Technology, University of Maryland, Baltimore County, Baltimore, Maryland

ARTHUR HOU

Laboratory for Atmospheres, NASA Goddard Space Flight Center, Greenbelt, Maryland,

(Manuscript received 23 March 2001, in final form 19 March 2002)

ABSTRACT

This paper assesses the impact of TRMM Microwave Imager (TMI) derived surface rainfall data on the numerical simulation of Supertyphoon Paka (1997). A series of mesoscale numerical simulations of Supertyphoon Paka is performed during its mature stage by using the Pennsylvania State University–National Center for Atmospheric Research (Penn State–NCAR) Mesoscale Model (MM5). The model initial and boundary conditions were derived from Goddard Earth Observing System (GEOS) global analyses with and without assimilation of the TMI surface rainfall data. Simulation results clearly demonstrate that the GEOS analysis with TMI rainfall data leads to an improved simulation of Supertyphoon Paka in terms of its intensity and kinematical and precipitation structures, because rainfall assimilation modifies the environment of the storm such that the initial conditions are more favorable for development of the storm.

Since a bogus vortex is often necessary for initialization of typhoon (hurricane) simulations, additional numerical experiments are also performed by introducing mesoscale bogus vortices into GEOS analysis at the initial time using a four-dimensional variational technique. Simulation results indicate that a well-designed bogus vortex can play a dominant role in the improvements of forecasts of typhoon intensity and track. However, incorporation of the TMI data with a bogus vortex is still beneficial because it improves the simulation of the asymmetric storm structure.

1. Introduction

It has long been recognized that accurate rainfall measurement over the Tropics is important for tropical weather and climate studies. Recent numerical studies have demonstrated that inclusion of rainfall data into numerical models can impact numerical weather forecasts (e.g., Krishnamurti et al. 1993; Zupanski and Mesinger 1995). However, accurate measurement of the spatial and temporal variations of tropical rainfall around the globe was a critical problem in meteorology until the recent launch of the Tropical Rainfall Measuring Mission (TRMM). During TRMM's expected six-year mission, its broad sampling footprint between 35°N and 35°S has been providing the first detailed and comprehensive dataset on the four-dimensional distribution of rainfall and latent heating over the vastly undersampled tropical oceanic and continental regions. TRMM offers a unique opportunity to improve the understanding of tropical meteorology and to evaluate the impact of rainfall data on tropical weather forecasts.

Among tropical weather events, the tropical cyclone is one of the great challenges for numerical weather prediction because conventional observations are usu-

Corresponding author address: Dr. Zhaoxia Pu, NASA GSFC, Mail Code 912, Greenbelt, MD 20771.
E-mail: pu@agnes.gsfc.nasa.gov

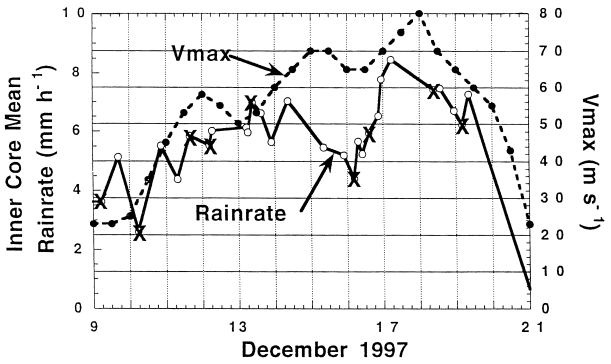

FIG. 1. Time series of Paka's estimated maximum wind speeds (dashed line, m s^{-1}) and SSM/I- (open circle) and TMI-derived (exes) mean inner-core (within 111 km of the center) rain rates (solid line, mm h^{-1}) for the period between 9 and 21 Dec 1997 [Courtesy of Rodgers et al. (2000).]

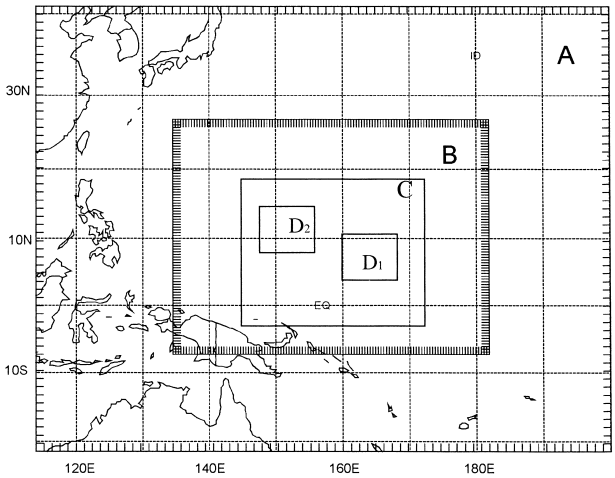

FIG. 2. Locations of the model domains for the simulation of Supertyphoon Paka (1997). Domain A is the 135-km grid, domain B the 45-km grid, and domain C the 15-km grid. Domain D is the 5-km grid and it is started at 24 h into the forecast. Domain D moves with the storm center, but the exact domain location may vary in the different experiments. For example, for experiment GEOSTRMM, domain D is moved from D_1 to D_2 between hours 24 and 72 of the forecast.

ally sparse over the tropical ocean. Therefore, it is necessary to incorporate satellite data into numerical weather prediction models. This study assesses the impact of TRMM Microwave Imager (TMI) derived surface rainfall data on the numerical simulation of Supertyphoon Paka, which was an event that was frequently sampled by TRMM in 1997 (Rodgers et al. 2000).

At the National Aeronautics and Space Administration's (NASA) Goddard Space Flight Center, the TMI-derived surface rainfall data have been assimilated into the Goddard Earth Observing System (GEOS) global analysis (Hou et al. 2000b). In order to examine the impact of TRMM data on numerical simulations of Paka, a set of mesoscale numerical simulations is performed during the storm's mature stage with the initial conditions generated by two different global analyses from the GEOS: one with and one without TRMM rainfall data. The fifth-generation Pennsylvania State University–National Center for Atmospheric Research (PSU–NCAR) nonhydrostatic regional Mesoscale Model (MM5), is used to conduct the mesoscale simulations. Details of the numerical results will demonstrate the impacts of the TRMM data on the simulations of Paka and identify how these impacts are associated with the rainfall data. In addition, because bogus vortices are often necessary for improving forecasts of mature tropical cyclones (Kurihara et al. 1993; Zou and Xiao 2000; Pu and Braun 2001), the numerical experiments are also performed by introducing bogus vortices generated by four-dimensional variational data assimilation (4DVAR) using the MM5 adjoint system. In one of the experiments, the bogus vortex is incorporated into the mesoscale initial conditions with the TMI data.

A brief overview of Supertyphoon Paka is given in section 2 and descriptions of the TMI surface rainfall data and GEOS data assimilation system are addressed in section 3. The mesoscale model and experimental design are described in section 4 and simulation results are given in section 5. A brief summary and discussion are provided in section 6.

2. Supertyphoon Paka

Supertyphoon Paka formed during the first week of December 1997 and underwent three periods of rapid intensification over the following 2 weeks. Rodgers et al. (2000) analyzed the detailed structural features of Paka during its lifetime using TRMM and the Defense Meteorological Satellite Program's Special Sensor Microwave Imager (SSM/I) satellite observations. Figure 1 shows Paka's intensity and SSM/I- and TMI-derived mean total inner-core (within 111 km of the center) rain rates for the period between 9 and 21 December 1997. Beginning early on 10 December, Paka's maxi-

TABLE 1. The model design.

Domain	Mesh A	Mesh B	Mesh C	Mesh D
Dimensions	72 × 56	118 × 88	202 × 169	202 × 169
Area coverage (km^2)	9 720 × 7 560	5 310 × 3 960	3 030 × 2 535	1 010 × 845
Grid size (km)	135	45	15	5
Time step (s)	360	120	40	13.3
Integration hours	0–72	0–72	0–72	24–72

TABLE 2. Experimental design.

Numerical expt	Model initial condition	Bogus vortex?
GEOS0	GEOS analysis without TMI rainfall	No
GEOSTRMM	GEOS analysis with TMI rainfall	No
BGS	GEOS analysis with TMI and bogus vortex	Yes
BGS0	GEOS analysis without TMI rainfall but with bogus vortex	Yes

mum wind speed increased from 23 to 58 m s^{-1} over a 48-h period with Paka becoming a mature category 3 typhoon on 11 December. Paka continued to intensify during the following days, and by 18 December, at the end of the last rapid deepening period, Paka became a supertyphoon with a maximum wind speed of about 80 m s^{-1}. In order to test the impact of the TMI rainfall data on the forecast of Paka during its mature stage, 0000 UTC 12 December 1997 is taken as the initial time for the numerical simulations in this study.

3. Surface rainfall data and GEOS rainfall assimilation

a. TMI surface rainfall data

The surface rainfall information is retrieved from the TMI microwave radiances by using the Goddard Profiling (GPROF) algorithm. The basis of the rainfall retrieval algorithm is the Bayesian technique described in Kummerow et al. (1996) and Olson et al. (1996, 1999). The GPROF scheme uses a database of simulated precipitation vertical profiles and the associated microwave radiances generated by a cloud-resolving model coupled to radiative transfer code (Tao and Simpson 1993; Wang et al. 2001). This database serves as a ''reference library'' to which actual sensor-observed radiances can be compared. Given a set of multichannel radiance observations from a particular sensor, the entire library of simulated radiances is scanned. The ''retrieved'' profile is a composite using profiles stored in a database that correspond to simulated radiances consistent with the observed radiances. A detailed description of the retrieval method utilized in the present study can be found in Olson et al. (1999).

For assimilation into the GEOS data assimilation system, the single-footprint instantaneous GPROF TMI surface rain rates are horizontally averaged to 2° latitude by 2.5° longitude grids, which are then time averaged over 6 h centered at analysis times (0000, 0600, 1200, and 1800 UTC). According to Hou et al. (2000b), the corresponding random error of the gridbox-averaged TMI rain rates is about 20%. Undersampling of the time-averaged rain rate over each 6-h analysis interval contributes additional error, approximately 20%–60%, depending upon the number of TMI overpasses within the interval.

b. GEOS analysis and rainfall assimilation

The 6-h averaged surface rainfall estimates derived from the TMI are assimilated into the global analysis using the GEOS data assimilation system (see Hou et al. 2000a). The analysis system uses the second generation of the GEOS general circulation model (GEOS-2 GCM, version 5.9) and version 1.5 of the optimal interpolation (OI) analysis scheme. The prognostic variables are potential temperature, specific humidity, surface pressure, and winds in the zonal and meridional directions computed at the resolution of 2° latitude, 2.5° longitude, and 46 σ levels from the surface to 4.0 hPa. A unique feature of the GEOS data assimilation system is that it uses the incremental analysis update (IAU) procedure of Bloom et al. (1996) to assimilate the rainfall and other observed data. The GEOS assimilation is a time-continuous model integration with a gradual insertion of IAU tendencies into prognostic variables updated from rainfall and other observations every 6 h. The system eliminates the general spinup problem in rainfall data assimilation. For rainfall data assimilation, Hou et al. (2000a,b) used a variational procedure in spatial and temporal (1 + 1D) dimensions based on a 6-h time integration of a column version of the GEOS global model with full model physics, with the advective terms prescribed from a preliminary 3-h assimilation using conventional observations. The 1 + 1D designation is used to distinguish it from 2D for two spatial dimensions. The general procedure of the scheme minimizes the least squared differences between the time-averaged TMI observations and rain rates generated by a column model averaged over a 6-h analysis window. The control variables are the analysis increments of moisture and temperature within the IAU framework of the GEOS analysis system. The 1 + 1D scheme, in its generalization to four dimensions, is related to the standard 4D variational assimilation algorithm but differs in its choice of the control variable: instead of estimating the initial condition at the beginning of the assimilation cycle, it estimates the constant IAU forcing to be applied over a 6-h assimilation cycle. Details of this procedure and the basic features of the 1 + 1D scheme are described in Hou et al. (2000a,b).

4. Numerical model and experimental design

a. MM5 model

The PSU–NCAR MM5 is used in this study to conduct numerical simulations of Paka. The MM5 is a limited-area, nonhydrostatic primitive equation model with multiple options for various physical parameterization schemes. The model employs a terrain-following σ ver-

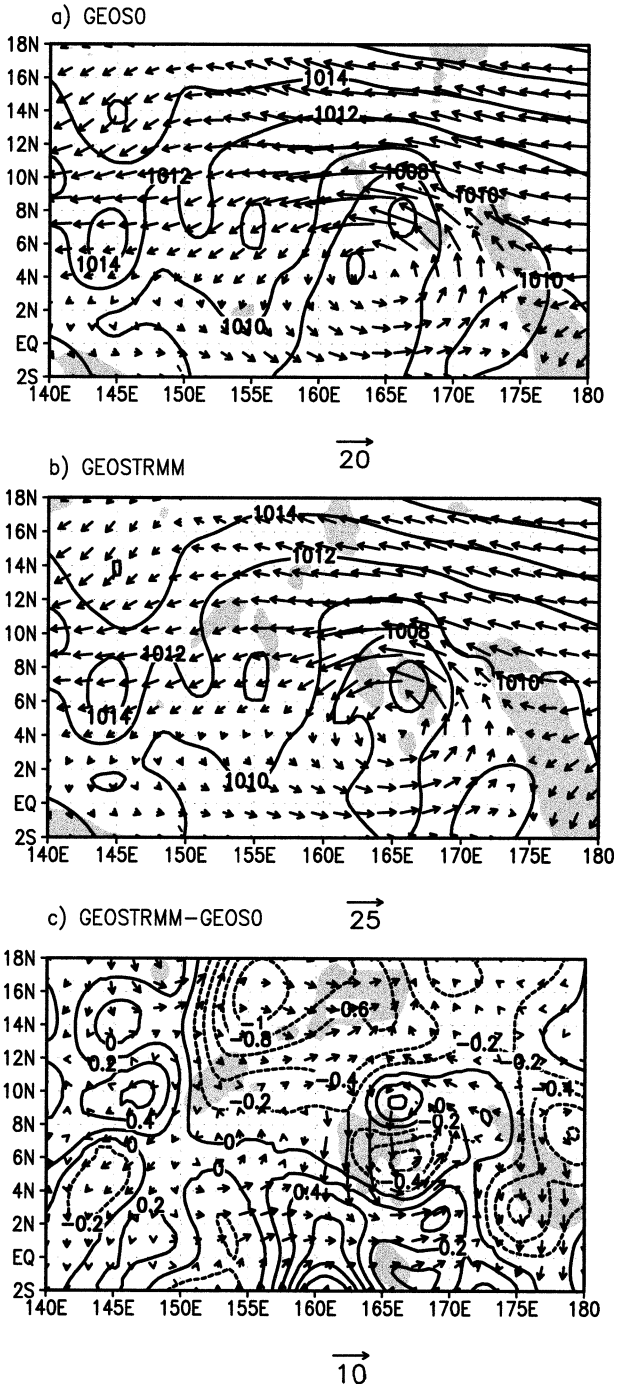

FIG. 3. Distributions of the initial SLP (contour interval, 2 hPa), horizontal wind vectors, and divergence (shading indicating divergence less than -7×10^{-6} s^{-1}) at 850 hPa in a portion of the 15-km domain for experiment (a) GEOS0 and (b) GEOSTRMM, and (c) the difference fields between GEOSTRMM and GEOS0. The wind vector scale is shown below each panel.

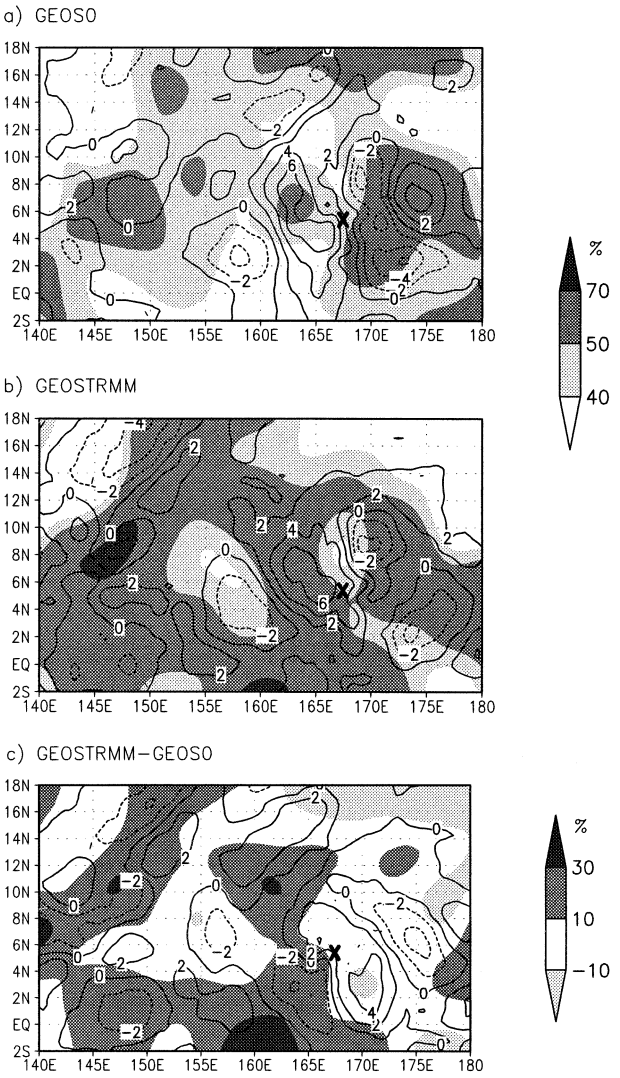

FIG. 4. The initial divergence (contour interval 2×10^{-5} s^{-1}) at 150 hPa and averaged 500–100-hPa relative humidity (shaded areas, %) for (a) GEOS0, and (b) GEOSTRMM, and (c) the differences between GEOSTRMM and GEOS0. The **X** denotes the position of the circulation center near the surface.

tical coordinate, where σ is defined as $\sigma = (p - p_{top})/(p_{sfc} - p_{top})$, p is pressure, and p_{sfc} and p_{top} are the pressures at the surface and model top, respectively. Physics options used for this study include the Betts–Miller cumulus parameterization, the Goddard cloud microphysics scheme (Tao and Simpson 1993), the Blackadar high-resolution planetary boundary layer parameterization scheme (Zhang and Anthes 1982), and the cloud atmospheric radiation scheme (Dudhia 1993). For a more detailed description of MM5, the reader is referred to Dudhia (1993) and Grell et al. (1995).

b. Experimental design

A two-way interactive, four-level nested grid technique is employed to achieve the multiscale simulation. Figure

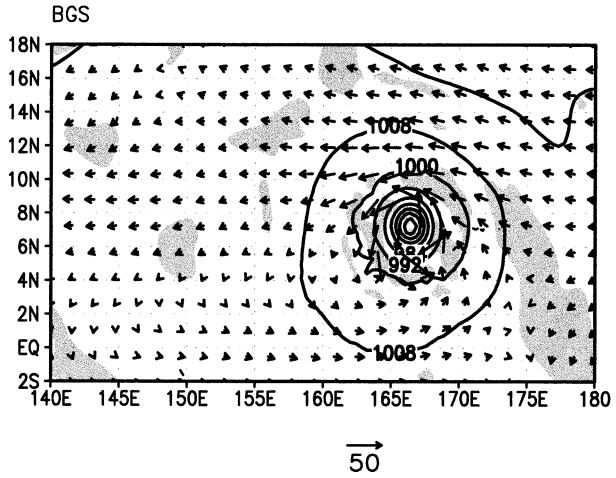

FIG. 5. Same as in Fig. 3a but for the initial conditions in experiment BGS with a contour interval for SLP of 8 hPa.

2 shows the four model domains used and Table 1 provides specifications for each domain. The outer domains A and B (135- and 45 km horizontal grid spacings) are fixed and are designed to simulate the synoptic-scale and mesoscale environment in which the system evolves. The sizes of the domains are chosen sufficiently large to minimize the influence of the lateral boundary conditions. The finer domains C and D (15- and 5-km grid spacings) are used to simulate the detailed hurricane-scale flows. The finest domain D is started at 24 h into the simulation and is frequently moved with the storm center (e.g., incrementally from D_1 to D_2) during the next 48 h of simulation. The model vertical structure comprises 27 σ levels with the top of the model set at a pressure of 50 hPa. The σ levels are placed at values of 1.0, 0.99, 0.98, 0.96, 0.93, and 0.89, and then decrease to 0.01 at an interval of 0.04. For the simulations, the model physics are the same for each domain except that no cumulus parameterization scheme is included for the 5-km domain.

c. Model initialization with GEOS analysis

For the experiments, the initial conditions for domains A and B are derived from 12-h GEOS analyses. In order to examine the impact of TMI data on the storm forecasts, two experiments (see Table 2) are conducted with initial conditions generated by two different sets of large-scale analyses from the GEOS: a control GEOS analysis dataset that does not include TMI rainfall data (GEOS0) and a second analysis dataset that does (GEOSTRMM). For initialization of grids A and B, the GEOS analysis fields (with and without the TMI data), including potential temperature, specific humidity, surface pressure, and the zonal and meridional winds, are interpolated horizontally to the meoscale model grid points. Following the MM5's preprocessing procedure, these interpolated analyses are refined by adding information from standard twice-daily rawinsondes and 3-h

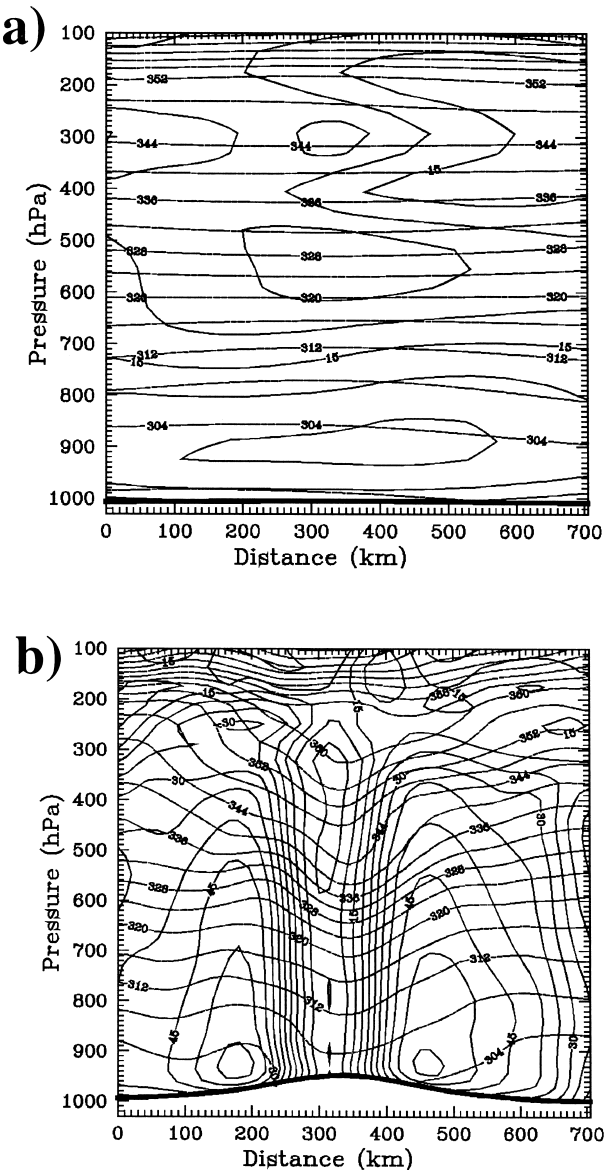

FIG. 6. East–west cross sections of initial potential temperature (4-K interval) and wind speed (5 m s^{-1} interval) through the center of the storms (corresponding to the centers in Figs. 3b and 5) for experiments (a) GEOSTRMM and (b) BGS.

surface and buoy reports using a Barnes objective analysis technique (Manning and Haagenson 1992). Final analyses are then interpolated to the model σ levels. The 15-km domain (domain C) is initialized by interpolation (see Grell et al. 1995) of all prognostic variables from the 45-km domain using a monotonic interpolation scheme based upon Smolarkiewicz and Grell (1992). Domain D is started at 24 h into the forecast and is initialized by interpolation of all variables from the 15-km domain. All figures in this paper present results from the 15- and 5-km grids.

Figure 3 shows the MM5 initial conditions for the GEOS0 and GEOSTRMM experiments (Figs. 3a and

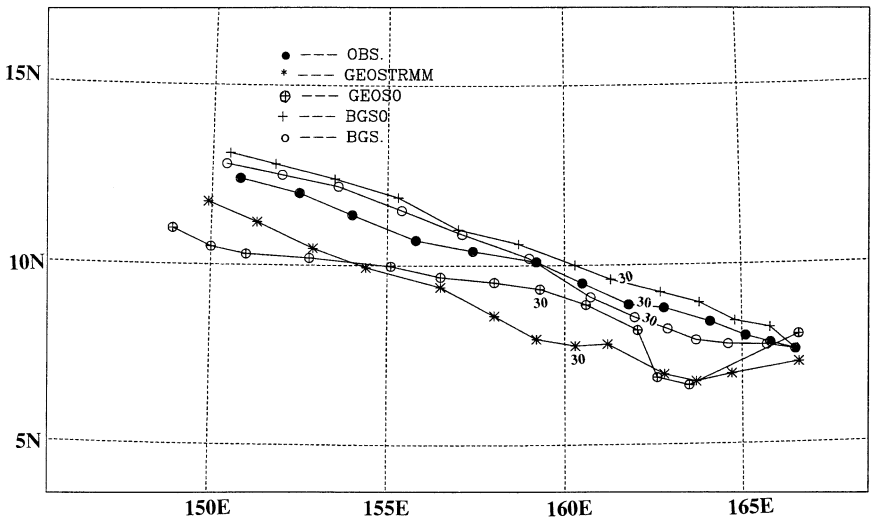

FIG. 7. Forecasts of the cyclone track for all experiments compared to the observed track. Center locations along the tracks are indicated every 6 h. The number 30 identifies the storm position at the 30-h forecast for each experiment.

3b) in a subset of the 15-km domain for fields of sea level pressure (SLP), 850-hPa wind vectors, and divergence at 0000 UTC 12 December 1997. At the time, Paka was a mature category 3 typhoon, but the figures show only a weak low pressure system with a broad wind speed maximum to the north and east of the circulation center. With assimilation of the TMI rainfall data (Fig. 3b), only slight differences (Fig. 3c) are found in the SLP compared with the case without TMI data, with the low near 7°N, 167°E being about 0.8 hPa deeper. Significant differences appear in the wind field with increases in wind speed of about 10 m s^{-1} on the western and southern sides of the convergence center (Fig. 3c). Low-level convergence is increased near the pressure minimum after insertion of TMI data into the initial condition and the center of the low pressure is shifted southward so that it is slightly more aligned with the circulation center (Figs. 3b and 3c).

Greater differences are observed in the upper-level divergence and humidity fields. Figure 4 shows the divergence field at 100 hPa and the averaged relative humidity between 500 and 100 hPa for initial conditions without (Fig. 4a) and with (Fig. 4b) the TMI data. The difference fields in Fig. 4c indicate that assimilation of the TMI data leads to a notable increase in relative humidity to the west of the storm and increased divergence over the storm in the upper troposphere (Fig. 4c). The greater humidity provides a more favorable environment for storm development, while the upper-level divergence, combined with increased low-level convergence, provides added forcing for upward vertical motions.

d. Bogus vortex

Since the initial conditions derived from the GEOS analyses contain a poor representation of the tropical cyclone vortex, additional numerical experiments are conducted in which a bogus vortex is introduced into the initial conditions. It has been shown that bogus vortices are helpful for tropical cyclone simulations (Kurihara et al. 1993; Leslie and Holland 1995). Zou and Xiao (2000) proposed a technique that assimilates bogus vortex information using four-dimensional variational data assimilation 4DVAR) methods. The method requires two steps: 1) specification of a bogus vortex by defining the position, radius of maximum surface wind (RMW), and minimum SLP of the initial vortex, and prescribing a symmetric SLP distribution over the vortex region; and 2) assuming that the time tendency of SLP is small in a short time period and then assimilating the specified bogus SLP field into the numerical model within a 30-min assimilation window. They (Zou and Xiao 2000) demonstrated the capability of this technique by using the MM5 adjoint system (Zou et al. 1998). Pu and Braun (2001) evaluated this technique and found that the wind information was required to ensure gra-

TABLE 3. Time series of the forecasted track error (km) for the four experiments.

Forecast time (h)	0	6	12	18	24	30	36	42	48	54	60	66	72
GEOS0	53	288	307	231	247	284	280	309	264	320	336	348	315
GEOSTRMM	41	156	210	218	211	211	227	215	160	185	174	188	167
BGS	0	14	57	73	67	45	51	30	81	98	85	65	55
BGS0	0	45	50	67	60	90	70	80	95	112	95	85	75

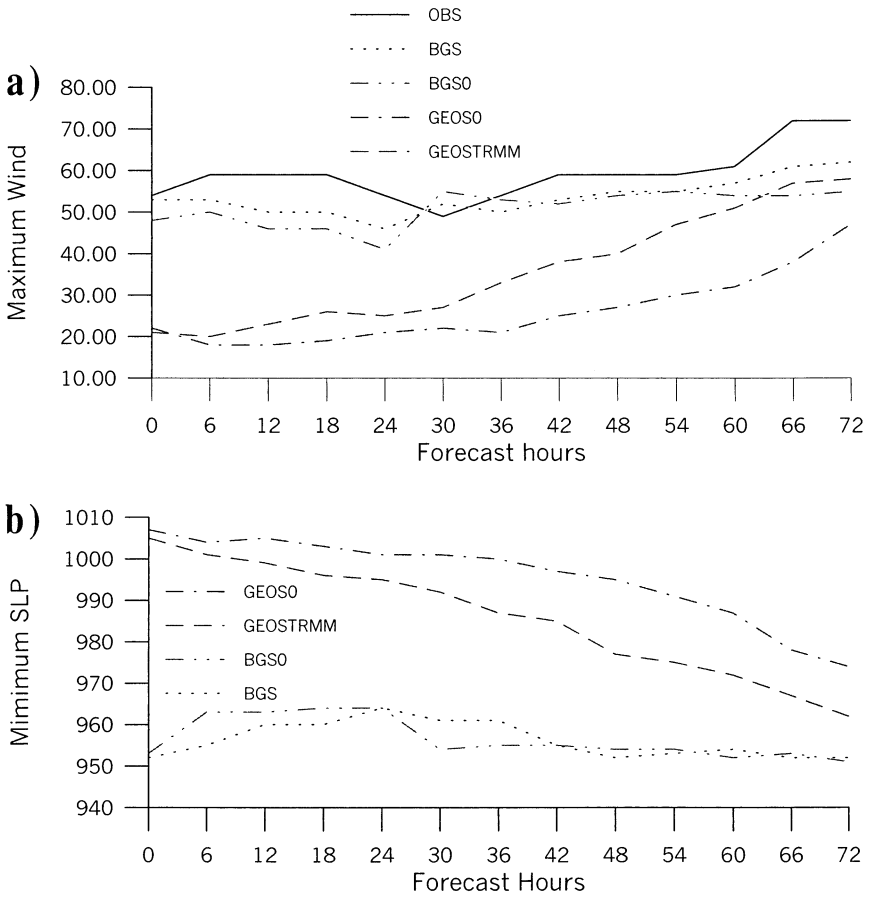

FIG. 8. Time series (at 6-h intervals) of (a) maximum winds (m s^{-1}) at the lowest model level (σ = 0.995, approximately 50 m) and (b) minimum SLP (hPa). Results during the period 24–72 h are from the 5-km grid forecast, while results at other times are from the 15-km grid.

dient wind balance, which helps to produce a better vortex structure and prevent vortex spindown problems. In this study, the vortex technique of Pu and Braun (2001) is used to generate the bogus vortex, with assimilation of the bogus vortex information applied only to the 45-km domain. Based upon the best available estimates, the parameters defining the bogus vortex are the following: storm central pressure of p_o = 955 hPa at the typhoon center (7.6°N, 166.5°E), an environmental pressure of p_n = 1012 hPa, maximum surface wind of V_m = 51.4 m s^{-1}, and RMW of R_m = 135 km. A large RMW is used because the 45-km grid spacing is inadequate for resolving the eye for realistic values of R_m. The bogus information extends out to a radius of 350 km for both SLP and tangential winds. The surface wind is extended into the vertical with a vertical profile following Kurihara et al. (1993). For the experiments, the specified SLP and wind information are assimilated every 5 min within a 30-min window. Similar to Pu and Braun (2001), the minimization procedure is stopped after 30 iterations. The initial conditions derived from 12-h GEOS analyses with (BGS) and without (BGS0) TMI rainfall, as described in the previous section, are taken as the first-guess fields for the 4DVAR system. Thus, for experiment BGS, the TMI rainfall information and mesosale bogus vortex data are incorporated together in the initial conditions. After assimilation of the bogus vortex, the 15-km nested domain is initialized by interpolation (see Grell et al. 1995) of all prognostic variables from the 45-km domain.

Figure 5 shows the SLP field and wind vectors and divergence at 850 hPa after the bogus vortex assimilation (BGS) for the 15-km domain. As expected, a strong vortex has been successfully introduced into the mesoscale initial fields. The intensity of the bogus vortex is close to the estimated intensity of Supertyphoon Paka. The vortex structure also extends throughout the troposphere. Figure 6 compares vertical cross sections of potential temperature and wind speed through the typhoon center before and after bogus data assimilation, showing that the temperature and wind structure are much improved with inclusion of the bogus vortex. A realistic wind structure and strong warm core feature near the typhoon center are well resolved in the initial conditions.

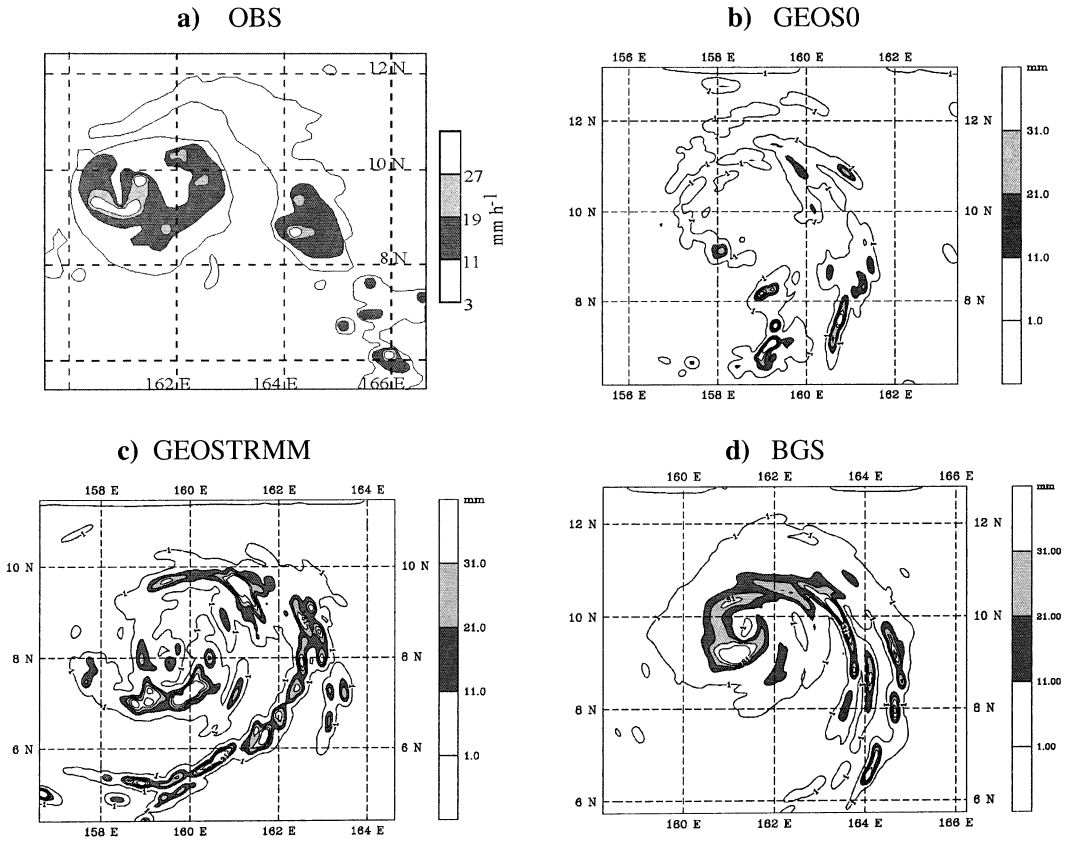

FIG. 9. Comparison of (a) the SSM/I-derived rainfall rate at 0911 UTC 13 Dec 1997 (OBS) with the forecasted 1-h-averaged rainfall rate (contour started at 1 mm h^{-1} with an interval of 10 mm h^{-1}) at 33 h (corresponding to 0900 UTC 13 Dec 1997) from the 5-km grid for experiments (b) GEOS0, (c) GEOSTRMM, and (d) BGS.

5. Simulation results

The numerical simulations of Paka are conducted for 72 h. Figure 7 compares the simulated tracks with the observed track for Paka. Results show that inclusion of the TMI data in the initial conditions slows the speed of the storm movement and improves the storm track (Table 3). However, this improvement does not sufficiently change the direction of storm movement so that the track errors remain large. The bogus vortex (BGS) results in significant improvement of the track forecast for Paka, partly because it improves the initial location of the vortex and also because it improves the interaction of the vortex with the environmental flow.

Figure 8 shows the temporal variation of maximum winds at the lowest model level (panel a) and the minimum SLP (or typhoon central pressure; panel b). The model winds are compared with estimates of the maximum surface wind derived from Dvorak (1975) techniques. No observed SLP information is available for comparison. Figure 8a shows substantial improvement of the maximum wind forecast when the model is started from the initial analysis with the TMI data compared to that without the TMI data. Although the differences between GEOS0 and GEOSTRMM are quite small at early times, significant differences develop after 6 h and even greater differences occur after 36 h as the storm in experiment GEOSTRMM becomes a typhoon and intensifies rapidly, while the storm in experiment GEOS0 undergoes much slower intensification and remains a tropical storm until 60 h. The numerical simulation with the bogus vortex provides a much better forecast in terms of both maximum wind and minimum SLP, comparing well with the estimated maximum wind information (Fig. 8a).

Figure 9 compares the SSM/I-derived rainfall rate (Wentz and Spencer 1998) at 0911 UTC 13 December (panel a) with the forecast 1-h accumulated precipitation at 33 h (corresponding to 0900 UTC 13 December) from the 5-km grid for experiments GEOS0 (panel b), GEOSTRMM (panel c), and BGS (panel d). At the time, Paka was a mature typhoon with a maximum surface wind of about 53 m s^{-1}. Significant differences among the rainfall forecasts are seen between the three experiments. Without assimilation of TMI rainfall data (GEOS0), the simulation produces only marginal pressure deepening with scattered rainfall around the low pressure system. With assimilation of the TMI rainfall (GEOSTRMM), the simulation produces a much more organized outer precip-

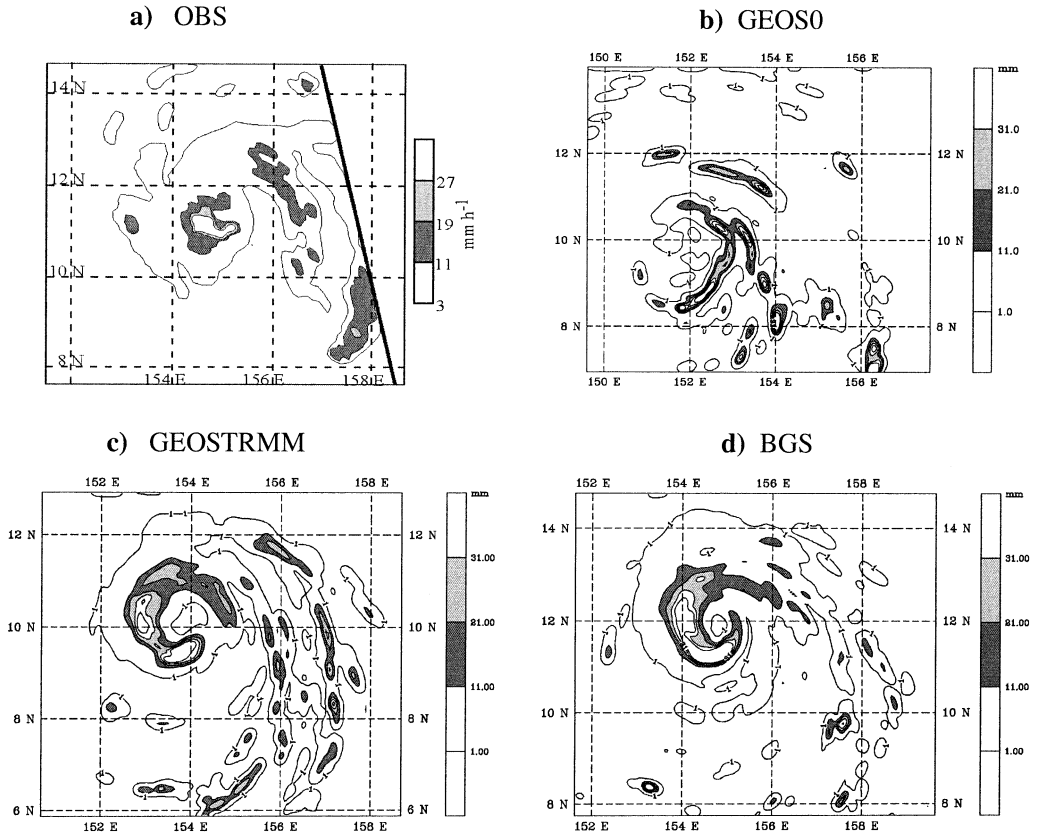

FIG. 10. Same as in Fig. 9 except valid for 0835 UTC 14 Dec 1997 and hour 57 of the forecast (corresponding to 0900 UTC 14 Dec 1997).

itation structure and a relatively strong tropical cyclone. The rainfall pattern reproduces the major features of the satellite-observed rainfall pattern, but an organized eyewall structure is generally lacking. With both TMI rainfall and the bogus vortex (BGS), the simulation produces the precipitation features that are consistent with the major observed features, including a well-defined eyewall and outer convective rainbands.

Figure 10 shows a similar comparison of the rainfall fields, but for the 57-h forecast. At this time, experiment GEOSTRMM (Fig. 10c) reproduces a mature typhoon with central SLP of 974 hPa and maximum surface winds of 45 m s^{-1}. The rainfall pattern matches SSM/I-derived rain features (Fig. 10a), showing the heavy precipitation on the western side of the typhoon eye and the multiple rainbands to the east. Similar features are also observed in experiment BGS (Fig. 10d) except that the intensity of the storm is even stronger. Without the TMI data included in the initial conditions, experiment GEOS0 remains a weak tropical storm and the precipitation pattern shows organized rainbands only on the eastern side of the storm (Fig. 10b).

Figure 11 compares the vertical structure of potential temperature and tangential wind speed fields within zonally oriented cross sections through the storm center at 57 h. Similar structural features are found in experiments GEOSTRMM and BGS, as they both produce strong tangential circulations and warm-core features in the eye. On the other hand, experiment GEOS0 shows a significantly weaker wind structure and warm core. Although the wind speeds (Fig. 11a) show a weak maximum near the center of the storm, indicating a weak eyewall structure, the overall intensity of the wind speed is much too weak. Only a very weak warm temperature anomaly appears in the upper troposphere.

Since the simulation results with the bogus vortex show significant improvement in the forecast of Paka, as a further comparison, an additional experiment (BGS0) is conducted in which a bogus vortex, with the same vortex parameters as in experiment BGS, was introduced into the GEOS analysis without assimilation of TMI data. The simulation results for experiment BGS0 show forecast impacts very similar to those in experiment BGS, with the storm track and intensity forecasts improved significantly (Figs. 7 and 8). These results suggest that the bogus vortex plays a dominant role in the forecasts of the mature typhoon in terms of its intensity and track. However, since the rainfall data were originally assimilated into a global model with coarse resolution, this conclusion should be confirmed in a future study by directly assimilating the rainfall data into the mesoscale model. While the BGS and

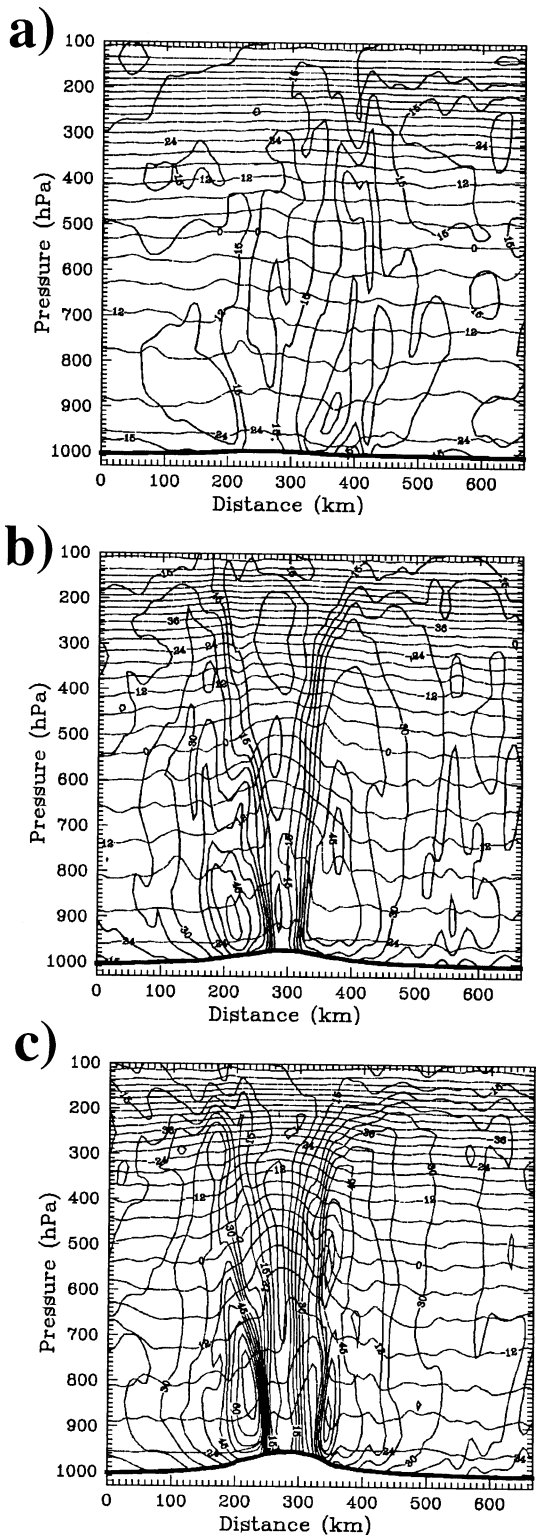

FIG. 11. East–west cross sections of the potential temperature (4-K interval) and wind speed (5 m s^{-1} interval) through the center of the storms (corresponding to the storm centers in Fig. 10) at 57 h for experiment (a) GEOS0, (b) GEOSTRMM, and (c) BGS.

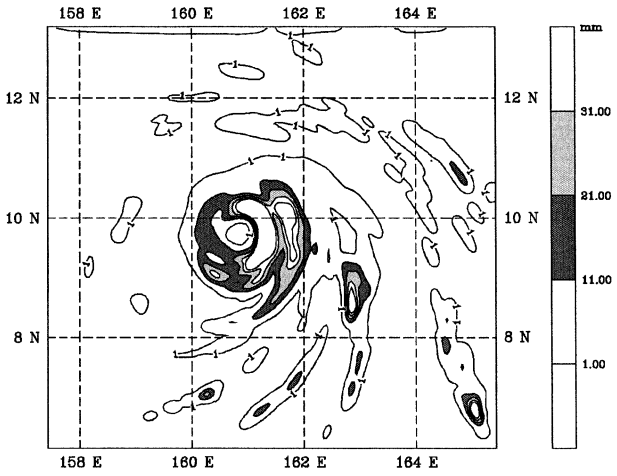

FIG. 12. Same as in Fig. 9d but for experiment BGS0.

BGS0 results are quite similar, Table 3 indicates that the track forecast in experiment BGS0 is slightly worse than that for experiment BGS after 24 h. Furthermore, distinguishable differences are observed in the precipitation structure between the two experiments during the first 36 h of the forecast. For instance, Fig. 12 shows the 1-h accumulated precipitation at 33 h from experiment BGS0, corresponding to the results in Fig. 9. Comparison of both bogus vortex simulations (Figs. 9d and 12) with the SSM/I observations (Fig. 9a) shows that experiment BGS produces a much more realistic precipitation structure. The improved precipitation structure in BGS is certainly attributable to the impact of including the TMI rainfall data in the initial and boundary conditions. The results also suggest that although the initial vortex can play a dominant role in the track and intensity forecasts of a mature typhoon, assimilation of rainfall data still brings some additional benefits to the forecast, especially to the short-term precipitation forecast.

6. Summary and discussion

Several numerical simulations have been conducted in order to examine the impact of assimilated rainfall data on forecasts of tropical cyclone structure and intensity. Results show significant differences among experiments with initial conditions derived from 1) GEOS analysis without assimilation of TMI rainfall, 2) GEOS analysis with assimilation of TMI rainfall data, 3) similar to point 1 above but including a mesoscale bogus tropical cyclone vortex, and 4) similar to point 2 but including a bogus vortex. The bogus vortex is assimilated into the initial conditions using 4DVAR techniques. The numerical results show the following.

- Assimilation of TMI rainfall data into the GEOS global analysis without the bogus vortex results in stronger low-level convergence and upper-level divergence, a

reduced initial SLP of the storm, and increased moisture in the upper troposphere. Rainfall assimilation thus modifies the environment of the storm such that conditions are more favorable for development. Consequently, the forecast of typhoon structure and intensity is improved significantly. The experiment with TMI data produces a storm of typhoon intensity after 36 h, while the simulation without TMI data requires 60 h to generate a typhoon.

- Since the GEOS large-scale analysis does not contain any mesoscale vortex information, further forecast improvements are obtained by combining the TMI rainfall data with a bogus vortex in the initial conditions. Inclusion of a bogus vortex and TRMM data in the numerical simulation produces a more accurate forecast of typhoon track and intensity, and a fairly accurate precipitation structure.
- The bogus vortex can play a dominant role in the forecasts of track and intensity of the mature typhoon. However, even with a bogus vortex, assimilation of the rainfall data into the model contributes beneficial impacts. For instance, in this study, it produces a better forecast of the eyewall precipitation structure, which implies an improved simulation of the vortex asymmetries.

This study has demonstrated the potential benefits of TRMM rainfall data on mesoscale numerical simulations of a mature typhoon. In this case, the rainfall data were assimilated into a large-scale analysis using a global analysis system and subsequently interpolated to the mesoscale grids. It is recognized that a preferred way to evaluate the impact of TRMM data on mesoscale simulations would be to assimilate the TMI rainfall data directly into the mesoscale model. Experiments with direct assimilation of the TMI rainfall data into the mesoscale model using 4DVAR techniques is in progress and will be reported on in a future study.

Acknowledgments. This work is supported by the NASA Headquarters Atmospheric Dynamics and Thermodynamics Program, and by the NASA TRMM project. The authors are grateful to Dr. R. Kakar (NASA/HQ) for his support of this research. Acknowledgment is also made to the NASA Goddard Space Flight Center for computer time used in this research. Comments from Dr. Ying-Hwa Kuo and two anonymous reviewers are also greatly appreciated.

REFERENCES

Bloom, S. C., L. L. Takacs, A. M. da Silva, and D. V. Ledvina, 1996: Data assimilation using incremental analysis updates. *Mon. Wea. Rev.,* **124,** 1256–1271.

Dudhia, J., 1993: A nonhydrostatic version of the Penn State–NCAR mesoscale model: Validation tests and simulation of an Atlantic cyclone and cold front. *Mon. Wea. Rev.,* **121,** 1493–1513.

Dvorak, V. F., 1975: Tropical cyclone intensity analyses and forecasting from satellite imagery. *Mon. Wea. Rev.,* **103,** 420–430.

Grell, G. A., J. Dudhia, and D. R. Stauffer, 1995: A description of the fifth-generation Penn State/NCAR Mesoscale Model (MM5). NCAR Tech. Note NCAR/TN-398 + STR, 138 pp. [Available from NCAR Publications Office, P.O. Box 3000, Boulder, CO 80307-3000.]

Hou, A. Y., D. V. Ledvina, A. M., Da Silva, S. Q. Zhang, J. Joiner, and R. M. Atlas, 2000a: Assimilation of SSM/I-derived surface rainfall and total precipitable water for improving the GEOS analysis for climate studies. *Mon. Wea. Rev.,* **128,** 509–537.

——, S. Q. Zhang, A. M. Da Silva, and W. S. Olson, 2000b: Improving assimilated global datasets using TMI rainfall and columnar moisture observations. *J. Climate,* **13,** 4180–4195.

Krishnamurti, T. N., H. S. Bedi, and K. Ingles, 1993: Physical initialization using SSM/I rain rates. *Tellus,* **45A,** 247–269.

Kummerow, C., W. S. Olson, and L. Giglio, 1996: A simplified scheme for obtaining precipitation and vertical hydrometeor profile from passive microwave sensor. *IEEE Trans. Geosci. Remote Sens.,* **34,** 1213–1232.

Kurihara, Y., M. A. Bender, and R. J. Ross, 1993: An initialization scheme of hurricane models by vortex specification. *Mon. Wea. Rev.,* **121,** 2030–2045.

Leslie, L. M., and G. J. Holland, 1995: On the bogussing of tropical cyclones in numerical models: A comparison of vortex profiles. *Meteor. Atmos. Phys.,* **56,** 101–110.

Manning, K. W., and P. L. Haagenson, 1992: Data ingest and objective analysis for the PSU/NCAR modeling system: Programs DATAGRID and RAWINS. NCAR Tech. Note NCAR/TN-376+IA, 209 pp. [Available from NCAR Publications Office, P.O. Box 3000, Boulder, CO 80307-3000.]

Olson, W. S., C. D. Kummerow, G. M. Heymsfield, and L. Giglio, 1996: A method for combined passive–active microwave retrievals of cloud and precipitation profiles. *J. Appl. Meteor.,* **35,** 1763–1789.

——, ——, Y. Hong, and W.-K. Tao, 1999: Atmospheric latent heating distributions in the Tropics derived from passive microwave radiometer measurements. *J. Appl. Meteor.,* **38,** 633–664.

Pu, Z.-X., and S. A. Braun, 2001: Evaluation of bogus vortex techniques with four-dimensional variational data assimilation. *Mon. Wea. Rev.,* **129,** 2023–2039.

Rodgers, E., W. Olson, J. Halverson, J. Simpson, and H. Pierce, 2000: Environmental forcing of Supertyphoon Paka's (1997) latent heat structure. *J. Appl. Meteor.,* **39,** 1983–2006.

Smolarkiewicz, P. K., and G. A. Grell, 1992: A class of monotone interpolation schemes. *J. Comput. Phys.,* **101,** 431–440.

Tao, W.-K., and J. Simpson, 1993: Goddard cumulus ensemble model. Part I: Model description. *Terr. Atmos. Oceanic Sci.,* **4,** 35–72.

Wang, Y., W.-K. Tao, J. Simpson, and S. Lang, 2001: The sensitivity of tropical squall lines to surface fluxes: Cloud resolving model simulations. *Quart. J. Roy. Meteor. Soc.,* in press.

Wentz, F. J., and R. W. Spencer, 1998: SSM/I rain retrievals within a unified all-weather ocean algorithm. *J. Atmos. Sci.,* **55,** 1613–1627.

Zhang, D.-L., and R. A. Anthes, 1982: A high-resolution model of the planetary boundary layer—Sensitivity tests and comparisons with SESAME-79 data. *J. Appl. Meteor.,* **21,** 1594–1609.

Zou, X., and Q. Xiao, 2000: Studies on the initialization and simulation of a mature hurricane using a variational bogus data assimilation scheme. *J. Atmos. Sci.,* **57,** 836–860.

——, W. Huang, and Q. Xiao, 1998: A user's guide to the MM5 adjoint modeling system. NCAR Tech Note TN-437+IA, NCAR/MMM Division. [Available from NCAR Publications Office, P.O. Box 3000, Boulder, CO 80307-3000.]

Zupanski, D., and F. Mesinger, 1995: Four-dimensional variational assimilation of precipitation data. *Mon. Wea. Rev.,* **123,** 1112–1127.